Jestr

Journal of Engineering Science and Technology Review 16 (3) (2023) 123 - 128

Lecture Note

JOURNAL OF
Engineering Science and Technology Review

www.jestr.org

Finite Element Study of Core Materials of a Planar Transformer and Comparison of its Electromagnetic Properties with a High Frequency Transformer

Arya Venugopal and Femi Robert*

Department of Electrical and Electronics Engineering, SRM Institute of Science and Technology, Kattankulathur-603203 Chennai, India

Received 14 March 2023; Accepted 30 May 2023

Abstract

In this work, an analysis of various soft magnetic materials that can be used as transformer core has been done to find the most suitable core material for a high frequency-operating planar transformer (PT). Using finite element analysis on a 2 kW, 100 kHz transformer, six soft magnetic core materials studied in this work are: cobalt-iron alloy, cold-rolled grain-oriented steel, carbon steel, koolmu powder, mu-metal and ferrite. The relative permeability of ferrite material was found to be of a moderate value of about 17000, which aids in decreasing the required magnetizing current and excess core losses due to eddy current generation. Also, the saturation magnetization value of ferrite was seen to be more than 0.2 T, which is high enough to prevent immature core saturation. Thus, it was concluded that ferrite material gave the best overall properties for the studied PT, thereby justifying its wide spread use in high frequency power electronics. Then, with this ferrite core material, electromagnetic properties like magnetic flux density of core and current density of windings of a PT and a conventional high frequency transformer (HFT) were analysed. From the magnetic flux density distribution of conventional HFT, it was seen that magnetic flux due to leakage increased the peak flux of the transformer to almost three times (about 0.9 T) that of the calculated peak flux density of 0.32 T. Whereas, the flux density distribution of the PT showed that most parts of the core operated at a flux value closer to the calculated 0.32 T, thereby making it a better design with lesser leakage flux losses. Also, when current density distributions were studied, it was observed that losses due to skin effects were lesser in PT by more than 60 % when compared to HFT.

Keywords: High frequency, Planar Transformer, Finite Element Modelling, Core Materials, Current Density, Magnetic Flux Density

1. Introduction

Nowadays, almost all emerging electrical and electronic components are required to enhance their performance with smaller size and increased outputs. High Frequency Transformers (HFTs) are becoming a crucial part of achieving this by supplying power at a high frequency to modern electronics. HFTs have the same basic operating principles as conventional line voltage transformers. As the name implies, the primary difference is that HFTs operate at a much higher frequency. That is, while most standard transformers operate at 50-60 Hz frequencies, HFTs work in frequencies ranging from 20 kHz to over 1 MHz [1]. The major advantage of operation of a transformer at high frequency is the reduced size obtained for the transformer. The higher the frequency, the smaller the transformer size can be, for a given power rating. But this benefit of lower profile and a higher power density poses challenges like increased core and copper losses due to associated skin and proximity effects of the windings [2].

Planar magnetic devices offer several advantages when compared to conventional magnetic devices. In a Planar Transformer (PT), the helical wire-wound structure of a conventional HFT is not employed. Instead, windings are placed on flat Printed Circuit Boards (PCBs) extending outward from the core [3], [4]. Thus, current distribution on the windings will be more uniform, resulting in reduced skin effects and thereby reduced copper losses in the windings [5]. Core losses in transformers are mainly due to unintended magnetic field distributions, causing eddy currents, along with excessive wire resistance and associated power loss. When there are air gaps in the core, stray magnetic flux lines extend in these gaps and induce undesired eddy current patterns in the core. On using planar magnetics, the magnetic flux density distribution is made more uniform throughout the core, as the core gaps are hugely reduced due to stacked accommodation of windings, PCB layers and insulators in a planar structure. Thus, core losses are reduced in PTs, along with other fringing effect losses due to air gaps [6].

Core material selection is a critical step in designing a transformer with high efficiency and power density, suffering minimal losses [7], [8]. Generally, one best core material cannot be singled out, since core material selection depends upon the application and topology of the system. But, several factors like magnetic field, relative permeability, saturation magnetisation etc. can be analysed to arrive at the better choices of core material for a specific topology. Proper selection of core material for a transformer can save the system from overheating due to core losses. Electromagnetic analyses were previously performed on transformers operating at high frequency with different advanced core materials like amorphous cores, nanocrystalline cores, air cores [9] etc. But a comparative analysis of core materials based on their electromagnetic properties was not done to find the better choices of core materials for high frequency applications.

Some relevant literature on high frequency transformers include analysis of their high power density and high efficiency performance. HFTs were designed for different scale microgrids based on high voltage insulation and

*E-mail address: r.femi85@gmail.com
ISSN: 1791-2377
doi:10.25103/jestr.163.16

transformer magnetic loss modelling [10]. Another work done previously on HFTs was building of a transformer loss model considering the magnetising current and fringing impact [11]. Finite Element Modelling (FEM) was used to analyse parasitic capacitances of windings of HFTs [12]. Efforts were made to design the basic construction of windings and core of HFTs to obtain desired high power density and efficiency characteristics [13], [14]. Several PT architectures were also developed over the years. A magnetic shunt integrated PT structure delivers a wider frequency range of operation for the system [15]. A matrix transformer structure based on variable width winding reduces the current stress and footprint of the transformer [16]. A paired layers winding structure minimises the common mode noise in PTs [17]. A fractional turns structure of PT ensures lesser volume and higher power density [18], [19]. Studies have been done even to analyse and model the high frequency fringing losses of PTs [6]. But a study of magnetic flux density and current density distributions were not included in any of these works to analyse the core and copper losses found in the transformer during its high frequency operation.

In this work, several core materials were studied using FEM simulations to identify the most suitable core material for the designed planar transformer. Properties like permeability, saturation magnetisation and magnetic fields were studied for all the materials. Also, phenomena like skin effect and fringing effect were studied on a conventional HFT and a novel PT using magnetic flux density distributions and current density distributions obtained using the FEM software Altair Flux, to analyse the benefits of planar-winding technology. This paper is divided into the following sections: section II analysis of various core materials on the PT, section III gives the study of magnetic flux density distributions of HFT and PT, section IV gives the study of current density distributions of HFT and PT, and finally Section V gives a conclusion of the work.

2. Analysis of Various Core Materials on the PT

The basic structure of the PT modelled in the simulations is shown in Fig. 1.

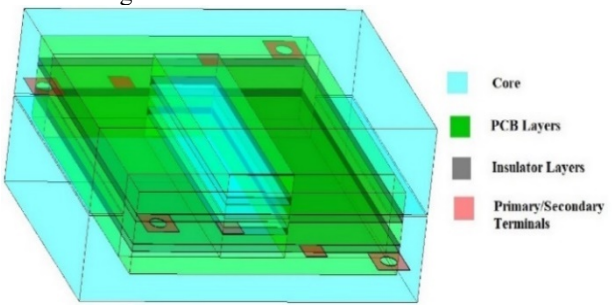

Fig. 1. Structure of the PT.

The PT is modelled as a simple EE core, designed with two window areas to accommodate the primary and secondary windings, insulations and printed circuit boards (PCBs). One E part of the core is placed on top of the other with a small air gap of 0.1 mm in between them. Such a small air gap will ensure that the fringing losses created by fringing fluxes in the air gaps are minimised. Other design specifications of the PT are given Tab. 1. The meshing structure used for the FEM simulations is shown in Fig. 2.

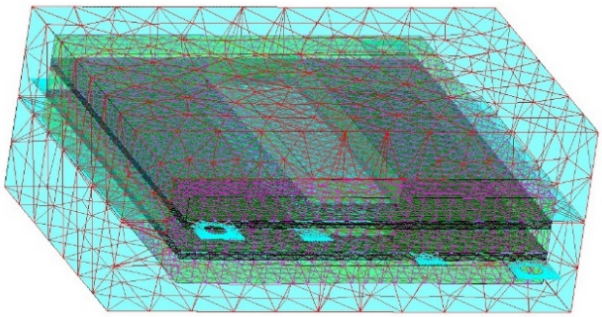

Fig. 2. Meshing structure of the PT.

To analyse various soft magnetic materials which are suitable as core material for a transformer operating at high frequency, modelling of the designed PT was done with 6 different materials; Annealed Cobalt-Iron Alloy, Cold-Rolled Grain Oriented Silicon Steel (or CRGO steel), Carbon Steel, Koolmu Powder, Mu-metal and Ferrite. The following properties were analysed for all the materials:

Table 1. Design specifications of the pt.

Specification	Value
Input Voltage	100 V
Load Rating	2 kW, 50 Ω
Frequency	100 kHz
Turns Ratio	2 : 3
Winding material	Copper
PCB material	Polyamide
Insulator material	Porcelain

2.1. Permeability

Permeability ('μ') is basically a measure of the ease with which a material can be magnetised. It is given by the ratio of magnetic flux density ('B') and magnetising force ('H'); that is:

$$\mu = \frac{B}{H} \tag{1}$$

Relative permeability should be high for a good transformer core material. This will help in reducing the core losses considerably, since a smaller magnetising current will be sufficient to produce required magnetic flux in the core.
Out of the 6 core materials chosen, it was observed that Mu-metal has the highest permeability and Koolmu powder has the lowest permeability. The decreasing order of the relative permeabilities of the 6 materials are given as below:

Mu-metal > CRGO steel > Ferrite > Co-Fe alloy > Carbon steel > Koolmu powder

But for high frequency operation, the relative permeability should not be too high. This is to maintain a balance between core and winding losses of the transformer.

2.2. Magnetic Field

The magnetic field, or current per area, is the primary factor that decides the suitability of a core material. It should be low for a good core material, so that the field is not too strong, thereby helping in reducing the core losses. The magnetic field distributions of the PT with the 6 different core materials chosen is shown in Fig. 3. It is seen that for all the 6 models, the magnetic field effects decrease from near the window areas

holding the current carrying windings, to the rest of the core. That is, the magnetic field is highest near the window areas with conductors, and gradually decreases towards farther areas of the core.

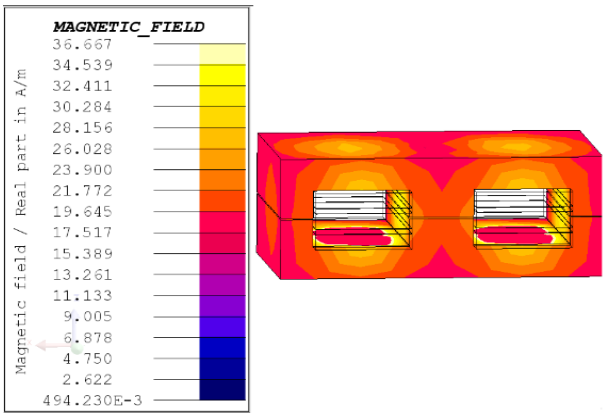

(a)

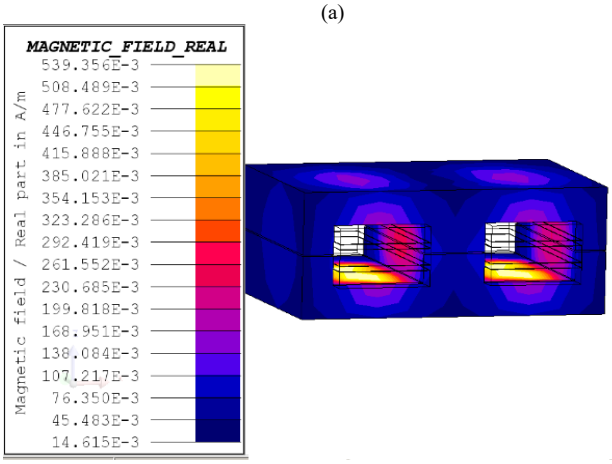

(b)

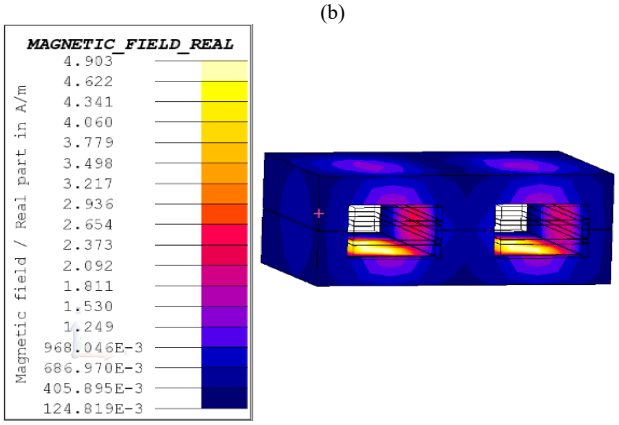

(c)

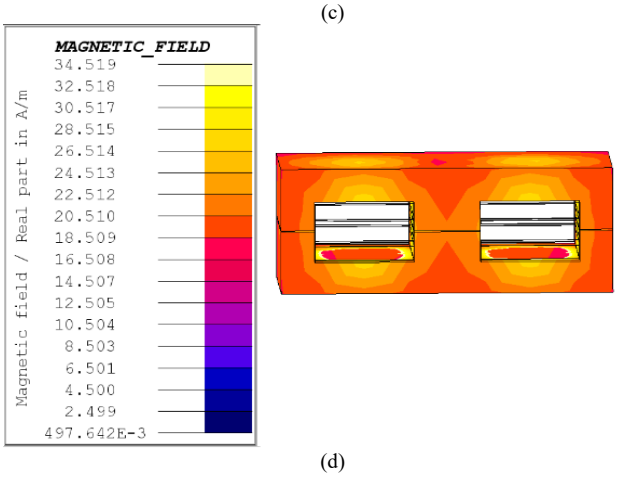

(d)

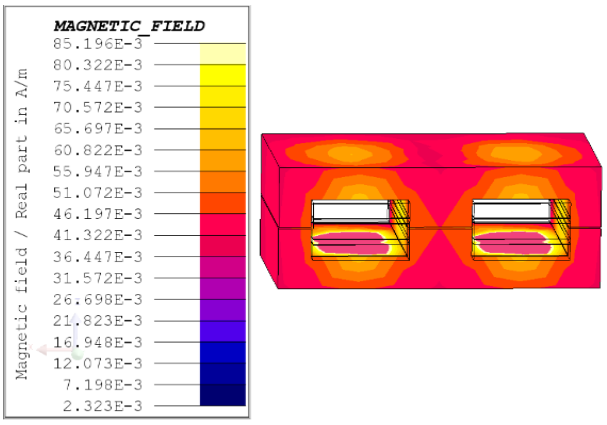

(e)

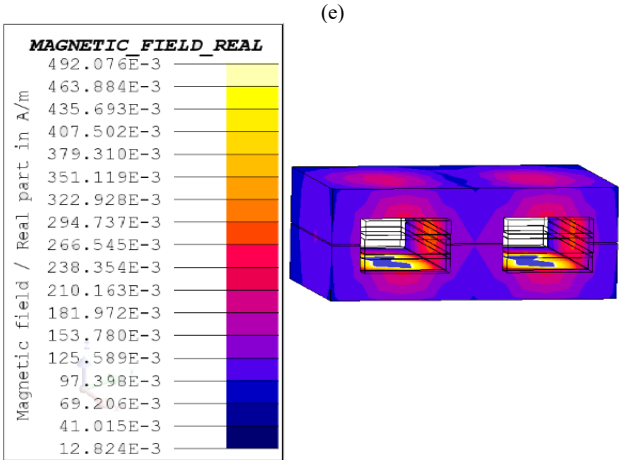

(f)

Fig. 3. Magnetic field distribution of (a) Annealed cobalt iron alloy core (b) Grain oriented silicon steel core (c) Carbon steel core (d) Koolmu powder core (e) Mu-metal core (f) Ferrite core.

Analysing the magnetic fields, it was observed that Koolmu powder has the highest magnetic field, and Mu-metal has the lowest magnetic field. Koolmu powder is an alloy of 6% aluminium, 9% silicon, and 85% iron, and Mu-metal is a nickel–iron soft ferromagnetic alloy with very high permeability [20]. The decreasing order of the magnetic fields of the materials compared are given as below:

Koolmu > Co-Fe alloy > Carbon steel > Ferrite > CRGO steel > Mu-metal

2.3. Saturation Magnetisation

Saturation magnetisation value of a good core material should be high. This is to prevent the core from saturating at low magnetic fields; that is, it is a measure of the strength of the core material to withstand high magnetic fields without saturating. If the core is saturated, then any more increase in magnetic flux density will not increase the magnetic field strength of the material. By studying the saturation magnetisation values of the 6 core materials chosen, it was observed that Ferrite core has the lowest saturation magnetisation value, and Co-Fe alloy has the highest saturation magnetisation value. The increasing order of the saturation magnetisation values of the 6 core materials are given as below:

Ferrite < Mu-metal < Koolmu < CRGO steel < Carbon steel < Co-Fe alloy

Tab. 2 gives the summary of analysis of various factors of the 6 different core materials. Analysing all the three factors, it can be found that the values of ferrite material and CRGO steel is the most optimum for core material, since it has a compromise value of all the required properties studied.

3. Study of Magnetic Flux Density Distributions of HFT and PT

Ferrite material was used for the core in both HFT and PT modelling. The structure and meshing of the HFT used for simulation are shown in Fig. 4.

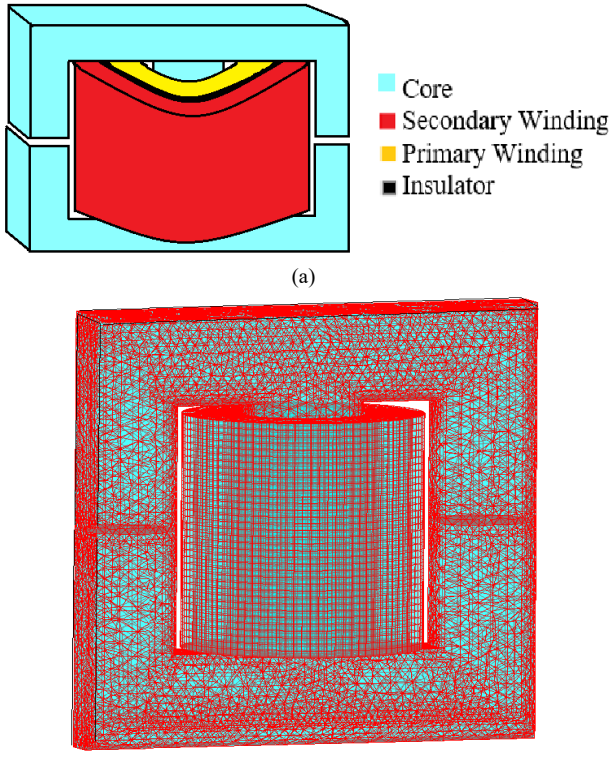

(a)

(b)

Fig. 4. (a) Structure of the HFT (b) Meshing diagram of the HFT

Table 2. Analysis of various factors for the 6 different core materials used.

Material	Magnetic Field	Relative Permeability	Saturation Magnetisation (T)
Co-Fe Alloy	21-23 A/m	3474	2.261
CRGO Steel	76-107 mA/m	35204	1.899
Carbon Steel	686-968 mA/m	1253	1.9
Koolmu powder	22-24 A/m	66.642	0.930102
Mu-metal	51-55 mA/m	74801	0.669
Ferrite	97-99 mA/m	17111	0.23968

For a sinusoidal wave input, the peak magnetic flux density 'B_{max}' of a power electronic transformer can be assessed with the formula [21], [22]:

$$B_{max} = \frac{V}{4.44 \times f \times N \times A_e} \quad (2)$$

where 'V' is the rms value of the input voltage (in Volts), 'f' is the frequency of operation (in Hertz), 'N' is the number of primary windings, and 'A_e' is the effective area of the core (in m^2). With a frequency of 100 kHz, area of 351 mm^2 [21], voltage of 100 V, and 2 primary windings, the calculated value of B_{max} was found to be 0.32 T.

The magnetic flux density distributions of the HFT and PT modelled are shown in Fig. 5. For both HFT and PT, the magnetic flux density values are seen to be larger in areas of core that are near to the windings and decreases at core areas away from the windings, as expected. This is also seen from the direction of magnetic flux density distributions of both HFT and PT shown in Fig. 6.

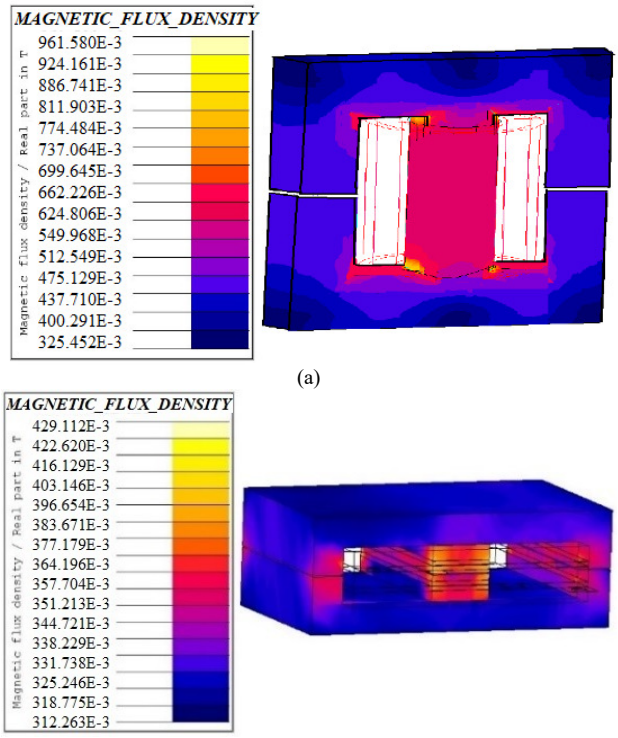

(a)

(b)

Fig. 5. Magnetic flux density distributions of (a) HFT (b) PT.

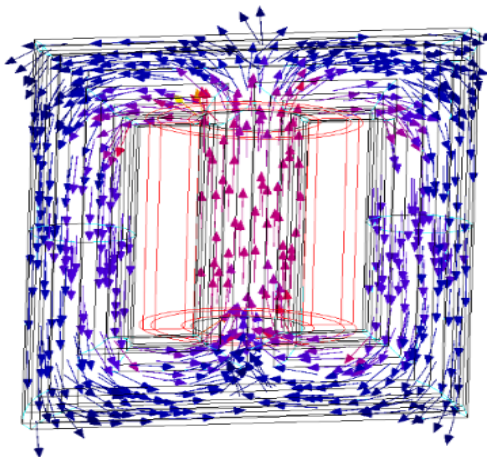

(a)

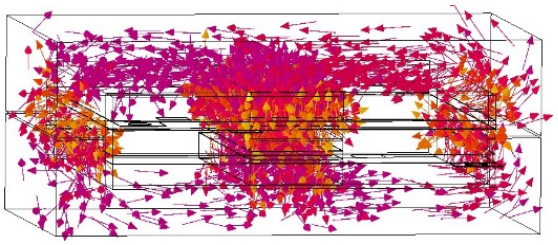

(b)

Fig. 6. Directions of magnetic flux density distribution of (a) HFT (b) PT.

In the magnetic flux density distribution of a conventional HFT shown in Fig. 5 (a), it is seen that most parts of the core have a magnetic flux density value much higher than the calculated B_{max} value of 0.32 T, whereas from the magnetic flux density distribution of the PT shown in Fig. 5 (b), it is observed that most parts of the core works at a flux density value closer to the calculated B_{max} value. A transformer is more optimised with lesser losses when it is working at a flux density value closer to its B_{max} value, thus making PT more optimised for losses than the conventional HFT. The larger leakage magnetic flux density seen in HFT is because of more gaps in the core and wire windings setup of an HFT. But these losses are lesser for a PT because of its planar arrangement of windings. Thus, by employing the planar winding structure of a PT than a conventional wire wound HFT structure, core losses of the transformer can be reduced for high frequency applications.

4. Study of Current Density Distributions of HFT and PT

Current density distributions of windings help in observing phenomenon like skin effect. Skin effect is basically the tendency of high frequency currents to concentrate towards the surface of conductors. Thus, current conduction will be concentrated more on the 'skin' of the conductors up to a definite 'skin depth'. Skin depth is the depth of conduction from the surface of the conductors. It is given as [5]:

$$\delta = \sqrt{\frac{\rho}{\pi \times f \times \mu}} \tag{3}$$

where 'ρ' and 'μ' are the resistivity and permeability of the conductor material respectively, and 'f' is the frequency of applied current. As it is seen from this equation, skin depth is inversely proportional to the frequency. So, during high frequency operation, skin depth will be very less, causing the whole of the current to be concentrated on a very small skin area of the conductor. The resistance 'R' of conductor is given by:

$$R = \frac{\rho\, l}{A} \tag{4}$$

where 'ρ' is the resistivity of the conductor material, 'l' is the length of the conductor, and 'A' is the area of conduction. So, as area of conduction is inversely proportional to conductor resistance, an increase in resistance is seen due to the decrease in area of conduction with skin effect. This will in turn increase the I^2R losses of the transformer during high frequency operation. Thus, skin effect has to be controlled, and a uniform distribution of current density has to be obtained throughout the conductor, so that there is no decrease in the area of conduction, and hence no increase copper losses of the transformer.

The current density distributions of both HFT and PT are shown in Fig. 7. The current density distribution of HFT as shown in Fig. 7 (a) is seen to be non-uniform, as the current density is observed to be much higher near the surfaces of the conductor due to skin effect. Whereas, from the current density distribution of PT shown in Fig. 7 (b), it is seen that there is a more uniform spread in current density. Thus, it is seen that copper losses due to skin effects is considerably reduced in employing PT for high frequency applications than using conventional HFTs.

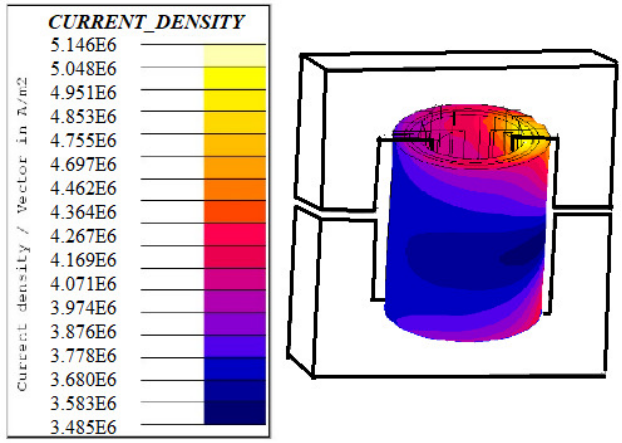

(a)

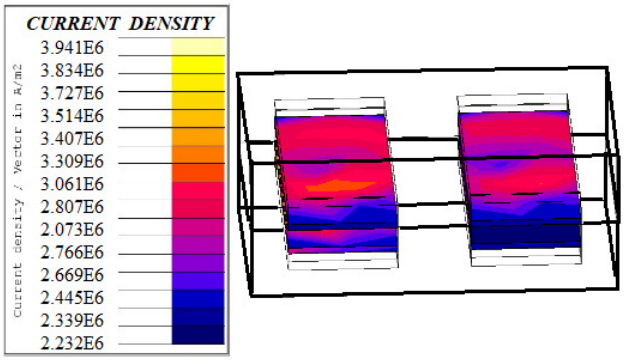

(b)

Fig. 7. Current density distributions of (a) HFT (b) PT.

5. Conclusion

In this paper, a study of decrease in losses obtained in using a novel PT than a conventional HFT for high frequency applications was done. When magnetic flux density distributions of both HFT and PT were simulated using FEM, it was seen that leakage flux losses were significantly lesser in the PT structure, and the flux density distribution was also more uniform in a PT than HFT. Similarly, when current density distributions of both HFT and PT were compared, it was seen that losses due to skin effect was considerably lesser in PT than HFT with a more uniform current density spread. Six different core materials were compared on a PT by analyzing parameters like magnetic field, relative permeability and saturation magnetization. It was seen that ferrite material and CRGO steel had the best properties for use as a core material in the designed PT.

Acknowledgments
This work is part of SRMIST Selective Excellence Research Initiative-2021: "DCFCEVB".

References

1. "Design Considerations for High Frequency Transformers," *Agile Magnetics*, 2021. https://www.agilemagco.com/blog/your-source-high-frequency-transformers/.
2. Bednarz C., Schreiber H., and Leone M., "Efficient Multiport Equivalent Circuit for Skin and Proximity Effect in Parallel Conductors With Arbitrary Cross Sections," *IEEE Trans. Electromagn. Compat.*, 60(6), 2018, pp. 2053–2056.
3. Zhang Z., Liu C., Wang M., Si Y., Liu Y., and Lei Q., "High-Efficiency High-Power-Density CLLC Resonant Converter with Low-Stray-Capacitance and Well-Heat-Dissipated Planar Transformer for EV On-Board Charger," *IEEE Trans. Power Electron.*, 35(10), 2020, pp. 10831–10851.
4. Ali Mamizadeh N. G., Bestoon Ahmed Mustafa, "Planar Flyback Transformer Design for PV Powered LED Illumination," *Int. J. Renew. Energy Res.*, 11(1), 2021 pp. 1-7.
5. Dixon L., "Designing Planar Magnetics," *Texas Instruments*, 2020. https://www.ti.com/download/trng/docs/seminar/Topic4LD.pdf.
6. Shafaei R., Perez M. C. G., and Ordonez M., "Planar Transformers in LLC Resonant Converters: High-Frequency Fringing Losses Modeling," *IEEE Trans. Power Electron.*, 35(9), 2020 pp. 9634–9651.
7. Ohodnicki P. R. and Bhattacharya S., "Finite-Element Analysis Modeling of High-Frequency Single-Phase Transformers Enabled by Metal Amorphous Nanocomposites and Calculation Winding Topologies," *IEEE Trans. Magn.*, 55(7), 2019, pp. 1–11.
8. Sarker P. C., Islam R., Guo Y., "State of Art Technologies for Development of High Frequency Transformers with Advanced Magnetic Materials," *IEEE Trans. Appl. Supercond.*, vol. 10, 2018, pp. 1-9.
9. Bai G., Gu C., and Lai L., "Electromagnetic Analysis of an Air-Core HTS Transformer," *IEEE Trans. Appl. Supercond.*, 29(2), 2019, pp. 1–3..
10. Zhao S., Shishuo, Li, Qiang, Lee, Fred C., & Li,, "High Frequency Transformer Design for Modular Power Conversion from Medium Voltage AC to 400V DC," *IEEE Transactions on Power Electronics,* 33(9), 2017, pp. 7545 - 7557.
11. Li B., Li Q., Lee F. C., and Fellow L., "High Frequency PCB Winding Transformer with Integrated Inductors for a Bi-directional Resonant Converter," *IEEE Trans. Power Electron.*, 34(7), 2019, pp. 6123-6135.
12. Sun Q. and Jiang F., "Modeling and Analysis of Parasitic Capacitance of Secondary Winding in High-Frequency High-Voltage Transformer Using Finite-Element Method," I*EEE Transactions on Applied Superconductivity*, 28(3), 2018, pp. 1–5.
13. Li G., and Wu X, "High Power Density 48V-12V DCX with 3D PCB Winding Transformer", In: *IEEE Applied Power Electronics Conference and Exposition (APEC),* New Orleanes, 2019, pp. 463-467.
14. Liu, Y.-C., Chen, K.-D., Chen, C., Syu, Y.-L., Lin, G.-W., Kim, K. A., & Chiu, H.-J.., "Quarter-Turn Transformer Design and Optimization for High Power Density 1-MHz LLC Resonant Converter," *IEEE Trans. Ind. Electron.*, PP(2), 2019, pp. 1-9
15. Li M., Ouyang Z., and Andersen M. A. E., "High-Frequency LLC Resonant Converter with Magnetic Shunt Integrated Planar Transformer," *IEEE Trans. Power Electron.*, 34(3), 2019, pp. 2405–2415.
16. Dai M., Zhang X., Li H., Zhou Di., Wang Y., and Xu Di., "LLC Converter with an Integrated Planar Matrix Transformer Based on Variable Width Winding," In*: 22nd Int. Conf. Electr. Mach. Syst. ICEMS 2019*, Harbin, China, 2019, pp. 1=4
17. Saket M. A., Ordonez M., Craciun M., and Botting C., "Improving Planar Transformers for LLC Resonant Converters: Paired Layers Interleaving," *IEEE Trans. Power Electron.*, 34(12), 2019, pp. 11813–11832.
18. Liu, Y.-C., Chen, C., Chen, K.-D., Syu, Y.-L., Lu, D.-J., Kim, K. A., & Chiu, H.-J., "Design and Implementation of a Planar Transformer with Fractional Turns for High Power Density LLC Resonant Converters," *IEEE Trans. Power Electron.*, 36(5), 2021, pp. 5191–5203.
19. Ranjram M. K. and Perreault D. J., "Leveraging Multi-Phase and Fractional-Turn Integrated Planar Transformers for Miniaturization in Data Center Applications," in *2020 IEEE 21st Workshop on Control and Modeling for Power Electronics (COMPEL)*, 2020, pp. 1–8.
20. Johan Kindmark F. R., "*Powder Material for Inductor Cores, Evaluation of MPP, Sendust and High flux core characteristics*." Department of Energy and Environment, Division of Electric Power Engineering, Chalmers University of Technology, 2013.
21. Marchio S., "Designing With the PLA51 Planar Transformer for Enhanced Power Density and Efficiency," in *Vishay Electronics-Transformer Application Note*, Vishay Sfernice Ltd., 2017.
22. Chapman S. J., "*Electric machinery fundamentals"*. Fifth edition. New York : McGraw-Hill, 2012 ©2012, 2012.